Biological Conservation 197 (2016) 190–199

Contents lists available at ScienceDirect

Biological Conservation

journal homepage: www.elsevier.com/locate/bioc

Developing population models with data from marked individuals

Hae Yeong Ryu [a], Kevin T. Shoemaker [a,1], Éva Kneip [a], Anna M. Pidgeon [b], Patricia J. Heglund [c], Brooke L. Bateman [b], Wayne E. Thogmartin [d], H. Reşit Akçakaya [a,*]

[a] Department of Ecology and Evolution, Stony Brook University, Stony Brook, NY 11794, USA
[b] Department of Forest and Wildlife Ecology, University of Wisconsin-Madison, Madison, WI 53706, USA
[c] U.S. Fish and Wildlife Service, La Crosse, WI 54603, USA
[d] U.S. Geological Survey Upper Midwest Environmental Sciences Center, La Crosse, WI 54603-1223, USA

ARTICLE INFO

Article history:
Received 25 September 2015
Received in revised form 19 January 2016
Accepted 26 February 2016
Available online xxxx

Keywords:
Population viability analysis
Stage-structured demographic models
Survival
Fecundity
Density-dependence
Monitoring Avian Productivity and Survivorship (MAPS)

ABSTRACT

Population viability analysis (PVA) is a powerful tool for biodiversity assessments, but its use has been limited because of the requirements for fully specified population models such as demographic structure, density-dependence, environmental stochasticity, and specification of uncertainties. Developing a fully specified population model from commonly available data sources – notably, mark–recapture studies – remains complicated due to lack of practical methods for estimating fecundity, true survival (as opposed to apparent survival), natural temporal variability in both survival and fecundity, density-dependence in the demographic parameters, and uncertainty in model parameters. We present a general method that estimates all the key parameters required to specify a stochastic, matrix-based population model, constructed using a long-term mark–recapture dataset. Unlike standard mark–recapture analyses, our approach provides estimates of true survival rates and fecundities, their respective natural temporal variabilities, and density-dependence functions, making it possible to construct a population model for long-term projection of population dynamics. Furthermore, our method includes a formal quantification of parameter uncertainty for global (multivariate) sensitivity analysis. We apply this approach to 9 bird species and demonstrate the feasibility of using data from the Monitoring Avian Productivity and Survivorship (MAPS) program. Bias-correction factors for raw estimates of survival and fecundity derived from mark–recapture data (apparent survival and juvenile:adult ratio, respectively) were non-negligible, and corrected parameters were generally more biologically reasonable than their uncorrected counterparts. Our method allows the development of fully specified stochastic population models using a single, widely available data source, substantially reducing the barriers that have until now limited the widespread application of PVA. This method is expected to greatly enhance our understanding of the processes underlying population dynamics and our ability to analyze viability and project trends for species of conservation concern.

1. Introduction

Assessing how close species are to extinction is one of the important first steps in preventing their extinction, which is a main goal of biodiversity conservation. One of the commonly used tools for making such assessments, as well as for evaluating the effectiveness of conservation actions, is population viability analysis (PVA). Using stochastic population demographic models, PVA projects population dynamics and calculates measures of viability such as extinction risk under current conditions and future changes in human impacts and management (Morris and Doak, 2002). Although uncertainties often exist, predictions made by PVA tend to be unbiased, contrary to subjective judgments made by experts, which makes it an effective tool in conservation science (McCarthy et al., 2004). Despite its advantages, the use of PVA is hampered by scarcity of reliable estimates of demographic parameters for most species. Mark–recapture data, collected by repeatedly capturing individuals that are uniquely and permanently marked at their initial capture (e.g., using tags or rings), continue to be of great value for estimating basic demographic parameters such as survival rates, abundance, and fecundities (Jolly, 1965). In addition to the rapid increase in the availability of long-term mark–recapture datasets for various taxa from geographically extensive and collaborative trapping efforts, new tools and methods for analysis of mark–recapture data enable more accurate and precise parameter estimation (Francis et al., 2014; King, 2012; Lindberg, 2012). Despite this progress, most mark–recapture analyses focus on estimating only survival parameters (Williams et al., 2002). Results from such analyses are useful for addressing a variety of ecological questions, but the general paucity of estimates for other demographic parameters, such as fecundity, temporal

* Corresponding author.
E-mail address: Resit.Akcakaya@stonybrook.edu (H.R. Akçakaya).
[1] Current address: Department of Natural Resources & Environmental Science, University of Nevada, Reno, Reno NV 89557.

http://dx.doi.org/10.1016/j.biocon.2016.02.031
0006-3207/

variability, and density-dependence in survival and fecundity, have hindered the development of fully specified population models that can be used to project future abundances and analyze population viability. Here, we explain the key elements that are required in building a population model and the common challenges for estimating such parameters.

1.1. Fecundity

Fecundity is a measure of the reproductive rate of an organism, species, or population and is defined as the per-capita number of offspring produced in each life history stage during a breeding season. From a population modeling perspective, fecundity estimates and survival estimates are both important; however the literature on estimating fecundity based on mark–recapture data is sparse in contrast to the vast literature on estimating survival. Fecundity estimates for birds have traditionally been obtained from nest surveys, in which the number of nestlings per nest or a similar quantity is measured. However, nest survey data require extensive field effort and are often unavailable. As an alternative, the ratio of juveniles to adults is conventionally used as an index of productivity (Flanders-Wanner et al., 2004; Peery et al., 2007). However, in population models, true fecundity, rather than an index, is required. The uncorrected juvenile:adult ratio is likely negatively biased, since juvenile birds and other wildlife are generally less observable than their adult counterparts. This bias can be corrected by using the ratio of capture probabilities between juveniles and adults, which are a byproduct of standard likelihood-based mark–recapture analysis (e.g., Cormack–Jolly-Seber model for estimating age-structured survival rates). In the context of population modeling, juvenile:adult ratio corrected in this way provides a superior estimate of population-level fecundity than estimates derived from labor-intensive nest surveys. Even when nest data are available, critical pieces of information, such as the proportion of breeding individuals in the population and the number of re-nesting attempts may not be available. Population models require fecundity to be estimated across all individuals in the population, including those that fail to produce eggs, and over all nesting attempts within a breeding season. If failed nests lead to additional nesting attempts, reproductive measures averaged over all observed nest attempts (such as fledglings per nest) underestimate fecundity. If only some individuals breed, measures such as fledglings per breeder overestimate fecundity, unless the population model explicitly models breeder and non-breeder stages separately and includes the rates of transition between them.

1.2. Survival

Survival rate is defined as the proportion of individuals of a given age or life stage in a population that survive from one breeding season to the next. Standard mark–recapture models for estimating survival do not distinguish mortality from emigration, and therefore estimate "apparent survival" (φ), which is the joint probability of surviving and remaining within the study area (and therefore available for recapture). However, survival and dispersal are distinct ecological processes that are almost always modeled separately in population models. Therefore, estimates of true, rather than apparent survival rates are needed. When all individuals are recaptured and their locations are known, multi-state or spatially explicit capture–recapture (SECR) methods can be used to estimate both survival and emigration rates (Ergon and Gardner, 2014; Schaub and Royle, 2014). Alternatively, if a dispersal kernel can be estimated, survival can be corrected for estimated dispersal out of the study area (Gilroy et al., 2012). However, when location information is not available, or its spatial resolution is too coarse to estimate dispersal rate, alternative approaches are required.

1.3. Temporal variability

Temporal variability in demographic parameters represents effects of unpredictable changes in the environment on population-level vital rates, and therefore, estimates of this variation are required for making stochastic projections. In all but the lowest abundance populations, environmental stochasticity exerts a greater influence on population-level risk metrics (e.g., extinction risk) than demographic stochasticity (Lande, 1993). Calculating unbiased estimates of temporal variability presents multiple challenges: first, it requires many years of data collection, and most importantly, one needs to separate sampling error from natural variability (also referred to as "process variance"). Although methods are available to estimate sampling error in survival from mark–recapture data (Gould and Nichols, 1998) and in both survival and fecundity from census data (Akçakaya, 2002), most studies do not use or describe in detail such methods. In addition to estimating process variance, sampling error determines uncertainty in model parameters, therefore, it must be used to estimate upper and lower bounds for model parameters to perform uncertainty analysis (e.g., sensitivity analysis; Chu-Agor et al., 2012; Curtis and Naujokaitis-Lewis, 2008).

1.4. Density

Negative feedbacks between vital rates and intra-specific densities are a key driver of abundance dynamics in most wild populations (Akçakaya et al., 1999; Burgman et al., 1993). Therefore, explicit specification of survival and fecundity rates across an ecologically realistic range of intra-specific densities is essential for most population modeling applications. Without explicit modeling of the density effects, the average stage matrix allows only very short-term projections, even if survival and fecundity are estimated over a long time period.

1.5. A comprehensive method

We present a comprehensive yet practical method for generating a fully specified, stochastic matrix-based population model based only on long-term mark–recapture data (Fig. 1). We used standard Cormack–Jolly–Seber (CJS) models to estimate stage-specific apparent survival rates (φ) and capture probabilities (p). We developed and applied several new approaches for generating unbiased estimates of fecundity (F), true stage-structured survival rates (S), temporal variability in survival and fecundity, and density-dependence functions for survival and fecundity. We used confidence intervals of parameter estimates to calculate parameter uncertainties for use in global (multivariate) sensitivity analysis. This method allows for estimating all parameters needed in a population model based on a single source of long-term mark–recapture data. This greatly eases the process of specifying a population model that would otherwise require additional independent datasets such as nest surveys and population count data.

2. Methods

2.1. Mark–recapture data: the MAPS project

We used mark–recapture data from the Monitoring Avian Productivity and Survivorship (MAPS) program (http://www.birdpop.org/pages/maps.php). The MAPS program, driven by collaborative effort among public agencies, non-governmental groups, and volunteers, comprises a network of ca. 1200 banding stations distributed across the US and Canada. Multiple mist nets are deployed at each station at least once per 10-day interval throughout the breeding period, where all newly captured birds are assigned to a unique band ID, all captures are identified to species, sex, and age (hatching year vs. adult), and multiple additional variables are recorded (e.g., mass, body condition). In MAPS, capture history data are now available for >180 species of land birds across North America. To demonstrate our approach, we selected 9 focal species that

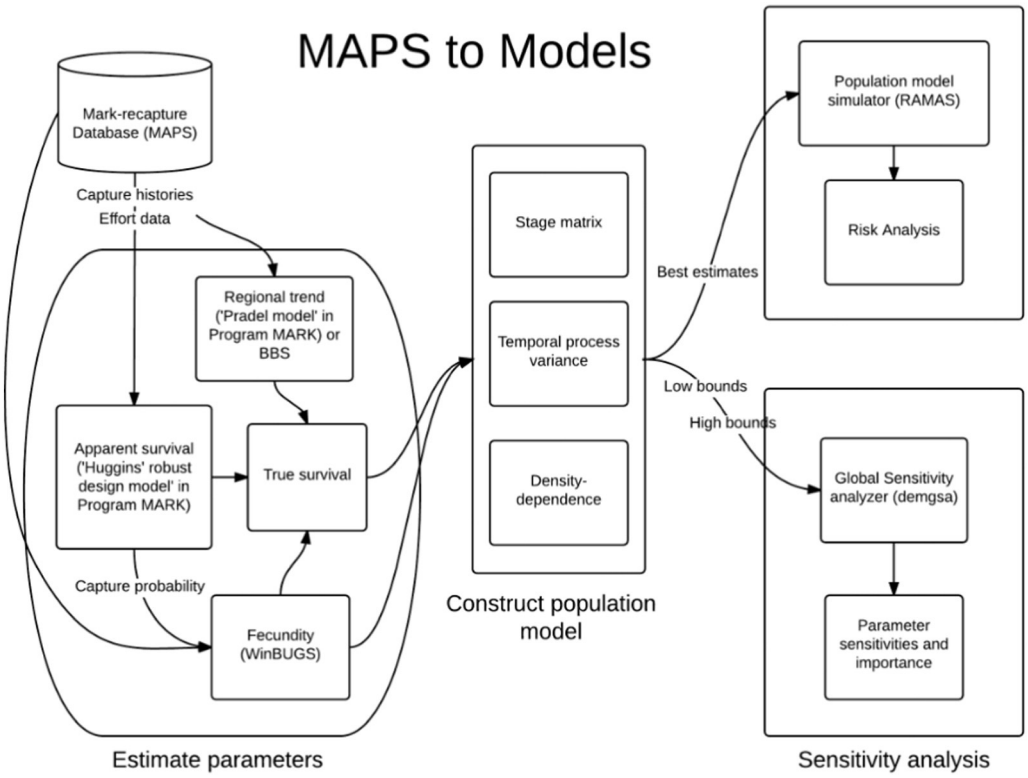

Fig. 1. Workflow diagram.

are geographically widespread and are commonly captured at banding stations (Table 1). The species represent a variety of life history traits (e.g., resident, migrant), foraging modes (e.g., canopy, mid-high, understory, ground), and diet specializations (e.g., invertebrate, fruit, seed, plant). To aid the determination of potential transients (important for survival estimation; see below), we extracted data on the status of the cloacal protuberance and the brood patch for all captured individuals in addition to band ID, date, banding station ID, and age. All analyses were based on capture records during the breeding season (May to August). We considered banding stations that were grouped together as "locations" in the MAPS network (generally comprising 1 to 7 stations) to be separate populations, in order to obtain time-specific estimates of relative density that is relevant for estimating the density-dependence relationships (see below).

2.2. Density

For density analysis, we used relative density. To calculate relative density, we first calculated the number of captured adults and juveniles, respectively, for each year, species, and population (MAPS location). We then corrected these numbers using adult and juvenile capture probabilities estimated from mark–recapture analysis. Finally, we computed relative density by dividing the sum of corrected abundances of adults and juveniles in each year by the average abundance over time for each population. Here, we assumed that adult and juvenile birds contribute equally to intra-specific competition for resources, therefore, summed the corrected abundances of adults and juveniles with equal weights. In order to match our analysis to how vital rates are used in most discrete-time population models, we specified survival from year t to $t + 1$ and fecundity in year $t + 1$ as functions of relative density in year t. We expected negative density-dependence relationships (survival and fecundity decreasing with increases in relative density) because positive density-dependence relationships (Allee effects) tend to be associated with populations characterized by abnormally low densities (Courchamp et al., 1999).

2.3. Effort

In order to standardize capture rates per unit effort, MAPS datasets include information on the duration of each mist netting event and

Table 1
Species list.

Species	4-Letter code	Resident/migrant	Foraging mode[a]	Diet[b]	# of total captures	# of unique capture histories
Black-capped chickadee (*Poecile atricapillus*)	BCCH	Resident	M,U	I,F,S	2735	2328
Carolina chickadee *Poecile carolinensis*)	CACH	Resident	M,U	I,S	2207	1954
Common yellowthroat (*Geothlypis trichas*)	COYE	Migrant	U,M	I	7403	5624
Gray catbird *Dumetella carolinensis*)	GRCA	Migrant	U,M	I,F	14,658	11,435
Hooded warbler (*Setophaga citrina*)	HOWA	Migrant	U	I	2812	2134
Northern cardinal (*Cardinalis cardinalis*)	NOCA	Resident	G,U,M,C	P,I,F	10,460	7942
White-eyed vireo (*Vireo griseus*)	WEVI	Migrant	U,M,C	I,P,F	8821	6452
Wood thrush (*Hylocichla mustelina*)	WOTH	Migrant	G,U	I,F	5738	4538
Yellow-breasted chat (*Icteria virens*)	YBCH	Migrant	U	I,F	2530	2012

[a,b]Foraging mode and diet are from Wilman et al. (2014).
[a] Foraging mode: C: canopy, M: mid-high, U: understory, G: ground.
[b] Diet: I: invertebrate, F: fruit, S: seed, P: other plant material.

the total number and dimensions of nets used. Such data are essential for refining capture probability estimates and thereby generating more accurate and precise estimates of population-level demographic rates (Cooch and White, 2006). For our analyses, we defined effort for each population as total net-days per month (standardized mist net was 12 × 2.5 m) across all banding stations.

2.4. Survival

Based on capture histories during the breeding season (May to August) in 1994–2012 (but 1994–2010 for black-capped chickadee because of low number of captures in 2011–2012), we estimated stage-specific apparent survival rates (φ) and capture probabilities (p; subsequently used to compute unbiased fecundity estimates; see below) using the Huggins' robust design model (Huggins, 1989, 1991) in program MARK (White and Burnham, 1999). Huggins' robust design model is an extension to the robust design model (Kendall and Nichols, 1995; Kendall et al., 1995, 1997) which allows the use of individual covariates. In our analysis, we used the Huggins' model to use individual covariates for capture probability (p).

We modeled two stages in the survival analysis (juvenile: <1 year; adult: ≥1 year). In our robust design model, years that represent discrete breeding periods were treated as primary capture occasions (among which populations were considered open to losses from mortality and emigration), and monthly intervals within years were treated as secondary capture occasions (among which the population was assumed to be closed). Because movement events are rare for breeding adults and hatching year birds during the breeding season, we applied this model to estimate capture probabilities (p) that were also used later to correct fecundity. All analyses were performed in the R environment (R Core Team, 2014) using the 'RMark' package (Laake, 2013).

Standard mark–recapture analyses often implicitly assume that all marked individuals are residents, therefore the presence of transients (defined as non-resident individuals that are available for capture for a single survey occasion) can result in survival rate estimates that are biased low (Hines et al., 2003; Nott et al., 2002; Pradel et al., 1997). To parse out the effect of transients, we estimated survival separately for individuals that can be transients ("potential transients"). Potential transients were identified as adult birds that were captured only once and observed in non-breeding condition (i.e., no observation of brood patch and cloacal protuberance) during the breeding season. In our analyses for survival, we included a covariate for potential transients which resulted in a separate apparent survival rate for an unknown mixture of transient and resident adults.

We constructed three models of apparent survival (φ): a "stage-model" to estimate time-constant survival, a "time-dependent model" for estimating temporal process variation, and a "density-dependent model" for estimating survival as a function of intra-specific density. In all models, φ was specified as a function of stage class (juvenile or adult) and status as potential transients (see above). For the "time-dependent model", φ was allowed to vary independently for each year and stage class (Table A.1). For the "density-dependent model", φ was modeled as a logit-linear function of relative density. We modeled capture probability (p) with additive effects of stage class (juvenile or adult) and effort (standardized net-days) (Table A.1).

The results from the time-dependent model provide a set of time-specific survival estimates separately for juveniles and adults. However, the total variance of the time-varying survival rates represents a mixture of sampling variance and process variance (Burnham and White, 2002). We used the variance components procedure implemented in Program MARK to isolate the process variance from the total variance, resulting in estimates of temporal stochasticity in apparent survival for adults and juveniles, respectively (Burnham and White, 2002; Gould and Nichols, 1998). If process variance was not separately identifiable in juveniles due to low number of captures, we used the estimate of adult process variance to compute juvenile process variance in survival, assuming that the coefficient of variation (CV) in survival among years was equal in juveniles and adults.

To estimate true survival (S), we increased the apparent survival estimates (φ) for both juveniles and adults such that the deterministic growth rate of the population model (the eigenvalue of the stage matrix, λ; the stage matrix used in our analysis is presented in 'Population Model') matched the estimated trend in population growth over the entire distribution for a given species (i.e. regional trend). Here, we assumed that the estimated regional trend is an unbiased representation of the overall population trend and that the disparity between the regional trend and the eigenvalue of the stage matrix is a result of underestimation of survival rates caused by marked individuals emigrating from study areas. In addition, we assumed that the level of disparity between apparent and true survival is the same in both juveniles and adults. To calculate λ, we used estimates of fecundity which resulted from our analysis (the method for estimating fecundity is described later in this paper). We obtained trend using the Pradel model ("reverse capture history" approach, Pradel, 1996) in program MARK which allows estimation of trend based on mark–recapture data without requiring abundance data (Cooch and White, 2006). By reversing the capture histories, the Pradel model is capable of estimating per-capita rate of entry into a population (analogous to apparent survival, φ) and population growth (Nichols et al., 2000). Here, we estimated a constant population growth rate (λ) across the study region by setting apparent survival (φ) constant (thus balancing the assumption of a constant growth rate, resulting in an unbiased estimate of λ) and modeling capture probability (p) as a function of effort.

Based on the trend estimate (λ) obtained from the Pradel model, we calculated true survival (S) for both adult (S_a) and juvenile survival rates (S_j) as:

$$S = \varphi\,(\lambda/\lambda_{app}), \tag{1}$$

where λ_{app} is the apparent finite rate of increase computed as $\varphi_a + \varphi_j * F$, and λ / λ_{app} is the "survival correction factor". In computing this correction factor, all apparent survival (φ) and fecundity (F; see below) terms were taken at mean values across all years and intra-specific densities. This "survival correction factor" can also be computed from any estimate of regional abundance trends, such as that reported by the North American Breeding Bird Survey (BBS) (Sauer et al., 2014). All survival rates presented in this paper were corrected using trend estimates derived from the Pradel model (described above); nonetheless, we tested and implemented an approach for using BBS trends to adjust survival rates (available in the source code; see Section 'Data accessibility').

Point (best) estimates for true adult (S_a) and juvenile survival (S_j) were computed simply by applying Eq. (1) to mean adult (φ_a) and juvenile apparent survival (φ_j) point estimates from Program MARK, respectively. To derive uncertainty bounds for S (e.g., for sensitivity analysis), we first applied Eq. (1) to all possible combinations of upper and lower bounds for the component terms φ_a, φ_j, λ, and F, derived respectively from Program MARK results (i.e., upper and lower 95% confidence bounds on φ terms), trend analysis (i.e., upper and lower 95% confidence bounds on λ estimated by the Pradel model or on the BBS trend), and the fecundity estimation process (upper and lower 95% credible interval from Bayesian posterior distribution of F). We then computed the upper and lower uncertainty bounds for S_a and S_j as the minimum and maximum values across all combinations of uncertainty bounds (although these bounds cannot be interpreted as a strict 95% confidence interval, which would almost certainly be narrower, this method was designed to provide reasonable lower and upper bounds for sensitivity analysis).

2.5. Fecundity

We estimated fecundity (defined as juveniles produced per adult per year) as the annual ratio of juvenile to adult captures at each defined

population (i.e. MAPS location), corrected for different capture probabilities between adults and juveniles. We assumed no age effects on fecundity for the species in our analysis. Estimated confidence intervals for capture probabilities of adults (p_a) and juveniles (p_j) were obtained directly from the survival analysis (results from Program MARK, see above).

The expected total number of juveniles produced ($\hat{N}_j$) in a population in each year was modeled as a log-linear function of relative intra-specific density with a lognormal random intercept term (γ_t) representing temporal process variance in fecundity.

$$\hat{N}_j = \exp\left(\log\left(\hat{N}_a\right) + \log(F_0) + \beta \cdot Density + \gamma_t\right), \quad (2)$$

where F_0 is the global mean fecundity for the species, $\hat{N}_a$ represents the true number of adult females in the population, β represents the log-linear fixed effect of intra-specific density (*Density*) on fecundity, and γ_t is a lognormal random intercept term representing the deviation from the mean fecundity in each year *t*. Here, the parameters that were estimated are mean fecundity (F_0), effect of relative density on fecundity (β), and temporal variance in fecundity (σ^2). Note that annual deviation from mean fecundity (γ_t) is in turn controlled by a single hyperparameter (σ^2) representing the (lognormal) temporal process variance in fecundity. This hierarchical parameter estimation scheme allowed us to directly estimate process variance (σ^2), in contrast with the post hoc method we used to estimate process variance in survival rates, and illustrates one of the reasons why ecologists are increasingly using hierarchical (often Bayesian) statistical models (Clark, 2005). The observed number of juveniles (N_j) was modeled as a Poisson random deviate with mean equal to the product of $\hat{N}_j$ and the probability of capture for juveniles (p_j). $\hat{N}_a$ entered the model as interval-censored data with upper and lower bounds defined by the equation ($\hat{N}_a = N_a / \mathrm{CI}(p_a)$), where N_a represents the observed total number of adult females captured within each population, and $\mathrm{CI}(p_a)$ represents the lower and upper 95% confidence bounds for adult capture probability extracted from the Program MARK results (time-dependent model, see above). Similarly, p_j entered the model as interval-censored data with upper and lower bounds defined by the 95% confidence interval for juvenile capture probability, extracted from Program MARK.

We also ran one variation on this model, the "uncorrected" fecundity model which omitted the capture probability (p) terms from Program MARK, using the raw observed numbers of juveniles and adults to estimate fecundity directly (analogous to the standard approach of using juvenile to adult ratio as a measure of fecundity).

We estimated all parameters with Markov chain Monte Carlo (MCMC) methods using WinBUGS 1.4 (Lunn et al., 2000), called from the R environment via the R2WinBUGS package (Sturtz et al., 2005). We assigned uninformative uniform prior probability distributions to all free parameters. We ran three independent Markov chains each with 1 000 000 MCMC iterations, discarding the first half as a burn-in and storing every hundredth of the remaining iterations for further analysis. We tested for convergence of the Markov chains to the stationary posterior distribution with the Gelman–Rubin diagnostic (Bolker, 2008). We diagnosed approximate convergence when the upper limit of the Gelman–Rubin diagnostic was ≤1.01. We summarized posterior distributions for all parameters with the mean of MCMC samples as a point estimate. To specify lower and upper uncertainty bounds (e.g., for sensitivity analysis), we used the 2.5 and 97.5 percentiles of the posterior distribution.

2.6. Population model

For each species, we created a population model with the best estimates of all model parameters. Using the estimates of survival rates (S) and fecundity (F), we developed a matrix-based population model with post-breeding census (Caswell, 2001):

$$\begin{vmatrix} F \cdot S_j & F \cdot S_a \\ S_j & S_a \end{vmatrix}.$$

Temporal process variance associated with each of the four matrix elements was also specified on the basis of the survival and fecundity analyses described above. The standard deviation of F was obtained directly from the fecundity analysis, where temporal (i.e. annual) variability in F was estimated as a free (hyper) parameter in the hierarchical model (hyperparameters of the γ_t term in Eq. (2)). Standard deviations of S_j and S_a were calculated using Program MARK's variance component analysis procedure (described above). To estimate the variance of $F \cdot S_j$ and $F \cdot S_a$ (the top row of the stage matrix), we used the formula given by Goodman (1960), assuming full correlation.

To accommodate uncertainty analysis, we computed lower and upper bounds for each of the stage matrix elements and associated temporal variability terms (Table 5). For the bottom elements of the stage matrix (S_j and S_a) and associated temporal variability terms, the lower and upper bounds were drawn directly from the survival analyses described above. We computed the uncertainty bounds of top row elements of the stage matrix (compounded fecundity and survival terms) by multiplying the respective lower or upper bounds of each component terms. For the uncertainty bounds on the variance terms, we applied the Goodman (1960) formula to the lower and upper-bound estimates.

Using the parameter estimates described above (survival rates, fecundity, and temporal variability and density-dependence functions associated with these vital rates), we developed population models, formatted both as generic text files and as input files for the population modeling software RAMAS Metapop (Akçakaya and Root, 2013). Separate files were generated for central point estimates ("best" estimates) and for upper and lower uncertainty bounds (lower and upper bounds for all parameters were packaged separately), which can be used to perform global sensitivity analysis with the new R package 'demgsa' (in review; https://github.com/mlammens/demgsa).

We did not model long-term change in average vital rates, although this can be added to our model for species with sufficient data to estimate a long-term trend. However, when vital rates are functions of population density (as they are in our models, and in any model developed for long-term projection), the important assumption is the long-term change in that relationship; specifically, the long-term change in the carrying capacity. Such change can be modeled with a time series of habitat maps based on changes in land-cover (Akçakaya et al., 2005) or climate (Fordham et al., 2013; Keith et al., 2008; Pearson et al., 2014). We also did not model long-term change in variability of vital rates. We are currently developing a method to incorporate changing environmental variance over time, using information on projected weather.

Since the functional forms of the density-dependence relationships in our survival and fecundity models are not among the standard functions used in population models, we implemented these in a compiled Dynamic Link Library (DLL), which is a program module that can be used or called by another (main) program. Because weak density-dependence combined with large temporal variability can push simulated abundances above plausible values, we implemented a restriction that truncates population sizes (i.e. relative density) at the maximum observed value for each population. The purpose of this is to prevent large densities from driving population dynamics, as we cannot be certain about the strength of the density-dependence mechanism beyond the observed density limits. Furthermore, it is reasonable to assume that at densities above the observed range, there are additional mechanisms of density-dependence (such as space limitations) that further limit population increases.

Unless otherwise specified, all analyses were performed in R (R Core Team, 2014); all scripts and functions for performing these analyses (Fig. 1), the MAPS data for the 9 species, and sample results can be freely downloaded via GitHub (see Section 'Data accessibility').

3. Results

We compiled a database comprising 57 364 capture records of 44 419 unique individuals (Table 1). Percentage of the individuals that were recaptured at least once varied from 10.6% (CACH) to 20.2% (NOCA). Adult recaptures were more commonly recorded than juvenile recaptures — the ratio of juvenile to adult recaptures varied from 0.14 (WOTH) to 0.84 (CACH).

Capture probability of adults and juveniles varied as a function of survey effort (Fig. 2). There were significant differences in capture probabilities between adults and juveniles for all species. Due to larger number of captures in adults, 95% confidence intervals for adult capture probability were substantially narrower than for juveniles (Fig. 2).

3.1. Fecundity

Average fecundity at mean density ranged from 0.58 to 4.07 juveniles per adult across the 9 species, and the temporal variability (standard deviation) ranged from 0.25 to 1.17 (Table 2). When fecundity was not corrected for different capture probability of adults and juveniles, the mean in fecundity was underestimated by 11% to 90% ('Bias in mean' in Table 2) and the temporal variability in fecundity was overestimated by up to 40% ('Bias in variability').

Except for WOTH and YBCH, fecundity was a negative function of density, although the density-dependence relationship was only weakly negative in most cases (Fig. 3a; Table A.4).

3.2. Survival

Average apparent survival rate (φ) at mean density ranged from 0.38 to 0.52 for adults and from 0.05 to 0.31 for juveniles across the species (Table 3). When φ was combined with the fecundity values, the apparent finite rate of population increase (Lambda, λ_{app}, in Table 3) ranged from 0.48 to 0.76. The finite rate of increase based on trend estimates (Lambda of trend, λ, in Table 3) ranged from 0.95 to 1.06. Increasing the survival rates so that the eigenvalue of the stage matrix matched the estimated trend resulted in true survival rates (S_a and S_j in Table 3) that were 1.3 to 2.0 times greater than the corresponding apparent survival rates (φ_a and φ_j in Table 3).

Table 2
Fecundity and its natural temporal variability (standard deviation, SD), with and without corrections for low juvenile capture probability.

Species	Fecundity (corrected for low juvenile capture probability)			Fecundity (not corrected)			Bias	
	Mean	SD	CV (%)[a]	Mean	SD	CV (%)	In mean (%)[b]	In variability (%)[c]
BCCH	1.14	0.66	58	0.671	0.41	62	−41	3
CACH	0.58	0.25	43	0.519	0.25	49	−11	6
COYE	1.66	0.63	38	0.321	0.13	40	−81	2
GRCA	4.07	1.17	29	0.424	0.12	29	−90	0
HOWA	1.93	0.94	48	0.214	0.09	42	−89	−7
NOCA	1.44	0.52	36	0.450	0.19	41	−69	5
WEVI	2.34	1.07	46	0.537	0.32	59	−77	13
WOTH	2.48	0.65	26	0.326	0.09	27	−87	0
YBCH	0.65	0.28	43	0.141	0.12	83	−79	40

[a] CV = SD/mean.
[b] [(mean of uncorrected F − mean corrected F) / mean of corrected F] * 100.
[c] CV of uncorrected F − CV of corrected F.

Only four of the species (BCCH, CACH, WEVI, and WOTH) exhibited negative density-dependence in survival (Fig. 3b; Table A.4). For other species, survival was a positive function of density, and therefore was modeled as density-independent (Table A.4; see Section '4. Discussion').

Overall, approximately half of the total variance in adult survival was due to sampling variability (estimated from a variance components analysis); process variance represented 32% to 60% of total variance, with a mean of 47% over the 9 species (Table 4). Except for NOCA and WEVI, process variance could not be estimated separately for juveniles because of small sample sizes (Table 4). Since the resulting temporal variability represents variation in apparent survival rates, we adjusted it by applying the same method used in correcting for true survival rates to get the temporal variability in true survival rates. Temporal variability in true adult survival rates (standard deviation) ranged from 0.07 to 0.21 (Table 4). If temporal variability in true juvenile survival rates could not be estimated due to lack of process variance estimates in juveniles, we estimated it by applying the coefficient of variation estimated for adults.

3.3. Population models

For each species, a population model was created using the best estimates of survival (S) and fecundity (F), their temporal variability, and their density-dependence functions. The resulting population models

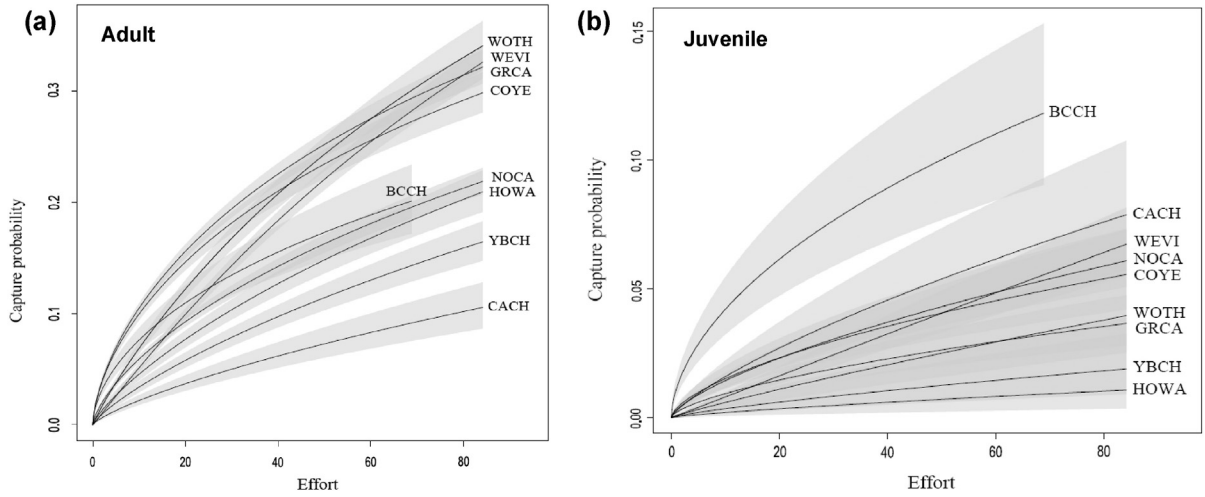

Fig. 2. Capture probability of (a) adults and (b) juveniles as a function of effort for the 9 study species. Gray areas indicate 95% confidence intervals. Effort is in units of total mist-net days per month.

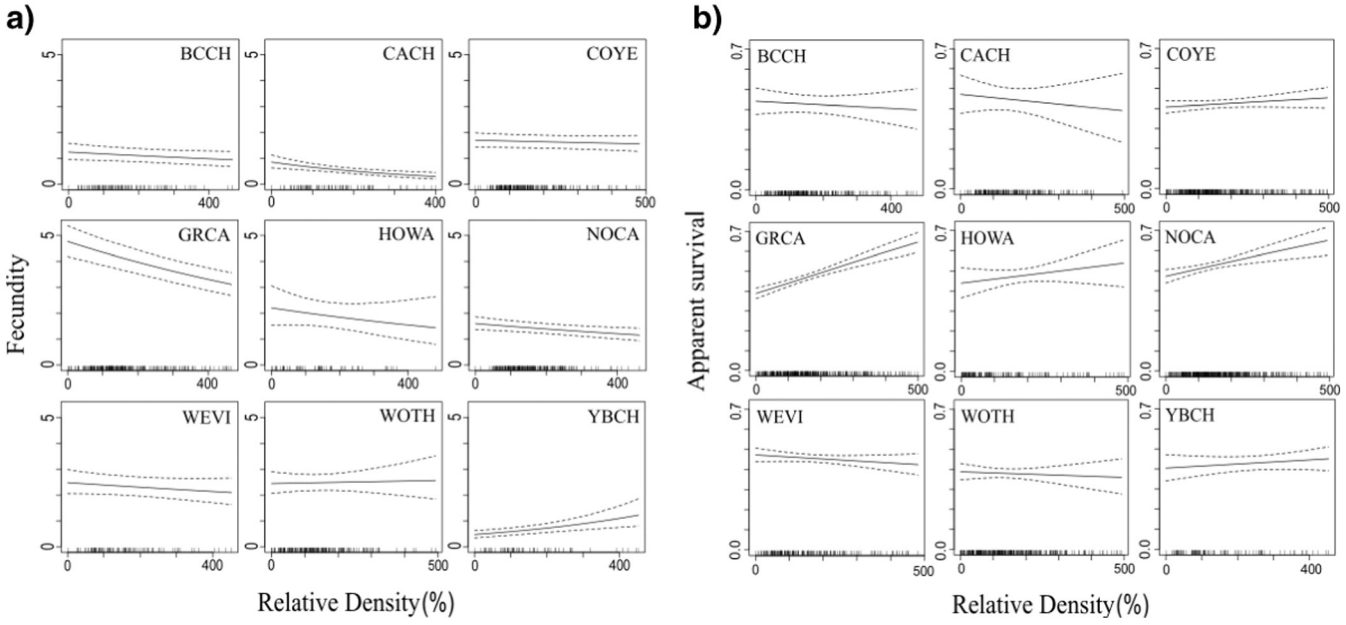

Fig. 3. (a) Fecundity and (b) adult apparent survival (φ) as functions of density for the 9 study species. Relative density is presented in % of the mean density over time. Rugs on x-axis represent observed values of relative density. Dotted lines indicate 95% CI.

simulated more realistic population trajectories than corresponding models that did not include the processes (stochasticity and density-dependence) and the corrections (for apparent survival and capture probability) that our approach implements (Fig. 4). For uncertainty analysis, we calculated the lower and upper bounds for each of the stage matrix elements and associated temporal variability terms. Estimates of the stage matrix elements and their temporal variabilities, and parameters of the density-dependence functions are given in Appendix A, together with their respective uncertainties (Tables A.2–A.6).

4. Discussion

Although population viability analysis is a powerful tool for biodiversity assessments, its use has been restricted because of data limitations. We demonstrated the feasibility of using a single source of data (i.e. mark–recapture) to develop a fully specified population model for viability analysis. Our approach estimates the four main elements required to model stochastic population dynamics: (i) unbiased fecundity estimates, (ii) true survival rates for adults and juveniles, (iii) temporal variability in these parameters (by separating out sampling error), and (iv) dependence of these parameters on population density. In addition, parameter uncertainties are incorporated for use in a global sensitivity analysis. If proper mark–recapture datasets are available, this approach can be readily applied to all types of mark–recapture analyses (e.g. data from camera traps) with some modifications in the models that fit the biology of the species modeled. By easing and facilitating the process of developing stochastic population models and sensitivity analysis, we believe our new approach has the potential to identify the

Table 3
Apparent and true survival rates of adults and juveniles.

Species	Apparent survival		Fecundity	Lambda	Lambda of trend	Corrected (true) survival	
	φ_a	φ_j	F	λ_{app}[a]	λ[c]	S_a	S_j
BCCH[b]	0.4298	0.1933	1.14	0.649	0.975	0.645	0.290
CACH[b]	0.4523	0.3117	0.58	0.634	0.995	0.710	0.489
COYE	0.4224	0.0798	1.66	0.555	0.957	0.729	0.138
GRCA	0.4710	0.0706	4.07	0.758	0.982	0.611	0.091
HOWA	0.4769	0.0833	1.93	0.638	1.058	0.7910	0.138
NOCA	0.5237	0.1476	1.44	0.736	1.007	0.717	0.202
WEVI[b]	0.4610	0.1128	2.34	0.725	1.027	0.653	0.160
WOTH[b]	0.3808	0.0499	2.48	0.504	0.996	0.752	0.098
YBCH	0.4295	0.0730	0.65	0.477	0.952	0.857	0.146

[a] Eigenvalue (λ) of the stage matrix using apparent survival rates.
[b] Survival rates based on density model. Except for these species, survival rates are based on the null model because the density model was biologically unrealistic.
[c] Growth rate corresponding to long-term trend in MAPS data, and the eigenvalue of the stage matrix using corrected survival rates.

Table 4
Temporal variability in survival rates of juveniles and adults.

Stage	Species	Total variance[a]	Process variance[b]	Sampling variance[c]	Temporal variability of apparent survival rate[d]	Temporal variability of true survival rate[e]
Juvenile	BCCH[f]	NA	NA	NA	NA	0.0800
	CACH[f]	NA	NA	NA	NA	0.1419
	COYE[f]	NA	NA	NA	NA	0.0172
	GRCA[f]	NA	NA	NA	NA	0.0112
	HOWA[f]	NA	NA	NA	NA	0.0329
	NOCA	0.00396	0.00099	0.00297	0.0315	0.0226
	WEVI	0.00187	0.00024	0.00163	0.0154	0.0204
	WOTH[f]	NA	NA	NA	NA	0.0136
	YBCH[f]	NA	NA	NA	NA	0.0342
Adult	BCCH	0.02786	0.01401	0.01385	0.1184	0.1778
	CACH	0.03806	0.01720	0.02086	0.1311	0.2060
	COYE	0.00887	0.00280	0.00607	0.0529	0.0913
	GRCA	0.00551	0.00333	0.00218	0.0577	0.0748
	HOWA	0.02293	0.01292	0.01001	0.1137	0.1885
	NOCA	0.00702	0.00343	0.00359	0.0585	0.0800
	WEVI	0.00761	0.00345	0.00417	0.0587	0.0832
	WOTH	0.00846	0.00278	0.00568	0.0527	0.1040
	YBCH	0.02013	0.01017	0.00996	0.1009	0.2012

[a] Based on time model in MARK.
[b] Estimated using variance component analysis.
[c] Total variance − process variance.
[d] If process variance was estimated, temporal variability in survival rate is the standard deviation of the estimated process variance.
[e] Standard deviation of survival rates corrected for the apparent survival which was calculated as coefficient of variation of apparent adult survival rate multiplied by true adult survival rate.
[f] Process variance could not be estimated due to low sample size, therefore, standard deviation is calculated as coefficient of variation of apparent adult survival rate multiplied by true juvenile survival rate.

Table 5
Stage matrix and standard deviation matrix for WEVI.

Stage matrix Mean (95% CI)	
0.374 (0.243–0.558)	1.528 (1.034–2.116)
0.160 (0.130–0.199)	0.653 (0.554–0.753)
SD matrix Mean (95% CI)	
0.218 (0.073–0.449)	0.892 (0.305–1.735)
0.020 (0.010–0.038)	0.083 (0.040–0.753)

underlying mechanisms driving present-day population dynamics and provide insights into the future conservation outlook for a wide range of common and at-risk species.

Recently, a framework called integrated population models (IPMs; not to be confused with integral projection models) has been developed to make inference about population dynamics using multiple independent datasets (e.g., capture-recapture data, nest surveys, population counts) (Schaub and Abadi, 2011). Using joint likelihoods, this new framework results in more precise parameter estimates, while enabling estimation of parameters that are otherwise not obtainable using only a single dataset (Abadi et al., 2010). By combining information that comes from multiple independent datasets, IPMs gain precision and therefore, have the advantage over the conventional methods that analyze each data separately (Schaub and Kéry, 2012). However, multiple independent sources of information are often unavailable for species of interest. Our method overcomes this problem and makes it possible to estimate all the parameters required for a matrix-based, stochastic population model from a single capture-recapture dataset. Because of this attribute, our framework is generally applicable to all other species that have only one source of long-term mark–recapture dataset.

Unlike conventional studies, our method successfully corrects the biases in parameter estimates, as demonstrated by the comparison between the corrected and uncorrected fecundity estimates for our study species. The independent analyses show that the uncorrected estimates of fecundity based on simple juvenile to adult ratio are unrealistically low. For example, for Gray Catbird (GRCA), 2.8 fledglings/nest and three broods per female is reported in the southeastern U.S. (Smith et al., 2011), resulting in 4.2 fledglings/adult. This is much higher than the uncorrected juvenile to adult ratio of 0.42, and similar to the corrected ratio of 4.07 (Table 2). For Northern cardinal (NOCA), fecundity is reported as 2.0–2.8 young fledged/pair/year (Halkin and Linville, 1999), corresponding to 1.0–1.4 fledglings per adult, which is much higher than the uncorrected juvenile to adult ratio of 0.45, and similar to the corrected ratio of 1.44. Furthermore, our hierarchical Bayesian method successfully removes sampling variance from the total variance of fecundity. This not only provides robust mean fecundity estimates but also the temporal variability term, which is a critical component of most stochastic population projection models. When simulated, our approach resulted in realistic projections of population dynamics compared to population models without these corrections (Fig. 4).

For survival rates and their variability, our approach adjusts the apparent survival rates derived from standard mark–recapture analysis so that the estimated population trend matches the regional trend of the species. This adjustment accounts for the difference between the apparent and true survival, i.e., emigration. This is not a direct estimate of emigration that would be useful for a dispersal model, because it represents emigration out of an undefined area. Directly estimating emigration rate would be the preferred method, but data from the MAPS program do not allow this (sparsely located MAPS stations make the detection of movement between stations impossible for most of the species). Hence, we used a practical approach based on the assumptions that (i) the regional trend is a reasonable, unbiased representation of the local population trend, (ii) the disparity between the estimated trend (or observed BBS trend) and the eigenvalue from the population model is a result of underestimation of survival rates (i.e. the difference between apparent and true survival), which in turn is a result of marked individuals emigrating from study area, (iii) the level to which the apparent survival differs from the true survival is the same in both juveniles and adults, and (iv) the fecundities are not underestimated. Evidence from independent estimates of fecundity (see above) suggests that this is a reasonable assumption to make; the resulting model is much more realistic than one using apparent survival instead of true survival, or those making an arbitrary assumption of emigration rate. Furthermore, there is no a priori reason to suspect that fecundity would be underestimated under our approach, whereas underestimation of survival rates (i.e., due to inability to distinguish mortality from permanent emigration) is a known issue that is especially likely to affect highly motile species such as songbirds.

Density-dependence is often a critical aspect of population models, not only because it strongly regulates the overall dynamics and affects the predicted risks of extinction, but also because it is often difficult to parameterize. With our approach, except for YBCH, we were able to fit a density model to either survival rate or fecundity, and for some species, both. It is not clear why we obtained positive density-dependence for some species in which the vital rate increased with increasing density. Allee effects might have played a role, but we believe it is highly

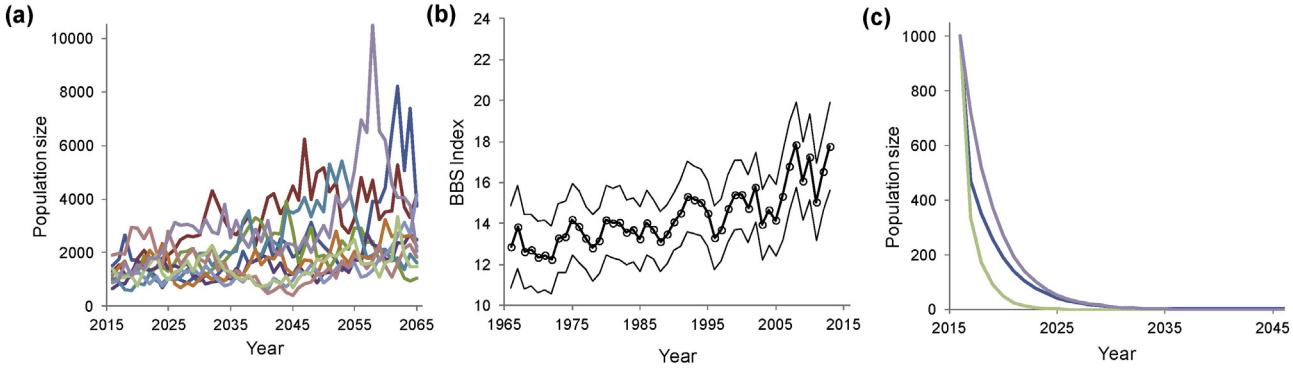

Fig. 4. (a) Projection of the stochastic population dynamics with the model developed for white-eyed vireo (WEVI). For clarity only the first 10 replicates are shown. (b) Breeding bird index for WEVI in the Southeastern Coastal Plain region (the FWS region with the largest number of survey routes on which the species was encountered). (c) Projection with the "naive" model that excludes stochasticity, density-dependence, as well as correction for apparent survival (top curve), correction for capture probability in calculating *F* (middle curve), and both corrections (bottom curve). Note the different scales used for (c) to allow visualizing the three curves.

unlikely that they caused the positive relationship over the entire observed range of population densities because Allee effects are mostly detected at low densities (Courchamp et al., 1999). Also, there is no evidence in the literature for Allee effects being particularly strong for these species. We believe that the cases of positive density-dependence represent limitations in the data, and therefore only implemented negative density relationships into the population models.

The datasets we used to test our approach included a wide range of sample sizes, approximately from 2000 to 15 000 total captures (Table 1). In general, our approach was applicable to all the datasets; the only issue we encountered with the smaller sample sizes was non-convergence in the time model for juveniles. Although we cannot be certain about the performance of our approach for sample sizes much smaller than about 2000 total captures, we believe that the major aspects of our approach (applying corrections to survival and fecundity and estimating density-dependence in both parameters) will not be overly sensitive to sample size.

Our study demonstrates the value of labor-intensive biodiversity monitoring programs such as MAPS which, by itself, provides sufficient amount of the data to develop a stochastic matrix-based population model. By requiring only a single long-term mark–recapture dataset, we strongly believe that this new method will ease the otherwise complex process of constructing a population model and enable future projections of population dynamics, especially for species for which mark–recapture data are the only source of information for estimating demographic parameters.

5. Data accessibility

MAPS data for the 9 species, the source code of the methods (R code for data formatting, R code for MARK analysis, WinBUGS, and density-dependence function), and sample results for one species can be freely downloaded via https://github.com/Akcakaya/MAPS-to-Models.

Acknowledgments

We thank the NASA Biodiversity Program and the Climate and Biological Response funding opportunity (NNH10ZDA001N-BIOCLIM) for support of this research. We thank the many volunteers who have contributed to the MAPS program and those who have run BBS routes. We also thank the Institute for Bird Populations for development and active curation of the MAPS dataset. Any use of trade, product, or firm names are for descriptive purposes only and do not imply endorsement by the U.S. Government. The findings and conclusions in this article are those of the authors and do not necessarily represent the views of the U.S. Fish and Wildlife Service.

Appendix A. Supplementary data

Supplementary material (Appendix A) is available online. The authors are solely responsible for the content and functionality of these materials. Queries (other than absence of the material) should be directed to the corresponding author. Supplementary data associated with this article can be found in the online version, at http://dx.doi.org/10.1016/j.biocon.2016.02.031.

References

Abadi, F., Gimenez, O., Arlettaz, R., Schaub, M., 2010. An assessment of integrated population models: bias, accuracy, and violation of the assumption of independence. Ecology 91, 7–14.
Akçakaya, H.R., 2002. Estimating the variance of survival rates and fecundities. Anim. Conserv. 5, 333–336.
Akçakaya, H., Root, W., 2013. RAMAS Metapop: viability analysis for stage-structured metapopulations. Version 6. Applied Biomathematics, Setauket, NY.
Akçakaya, H.R., Burgman, M.A., Ginzburg, L.R., 1999. Applied population ecology: principles and computer exercises using RAMAS EcoLab. second ed. Sinauer Associates, Sunderland, Massachusetts.
Akçakaya, H.R., Franklin, J., Syphard, A.D., Stephenson, J.R., 2005. Viability of Bell's sage sparrow (*Amphispiza belli ssp. belli*): altered fire regimes. Ecol. Appl. 15, 521–531.
Bolker, B.M., 2008. Ecological models and data in R. Princeton University Press.
Burgman, M.A., Ferson, S., Akçakaya, H.R., 1993. Risk Assessment in Conservation Biology. Chapman and Hall, London.
Burnham, K.P., White, G.C., 2002. Evaluation of some random effects methodology applicable to bird ringing data. J. Appl. Stat. 29, 245–264.
Caswell, H., 2001. Matrix Population Models. Wiley Online Library.
Chu-Agor, M.L., Munoz-Carpena, R., Kiker, G.A., Aiello-Lammens, M.E., Akçakaya, H.R., Convertino, M., Linkov, I., 2012. Simulating the fate of Florida snowy plovers with sea-level rise: exploring research and management priorities with a global uncertainty and sensitivity analysis perspective. Ecol. Model. 224, 33–47.
Clark, J.S., 2005. Why environmental scientists are becoming Bayesians. Ecol. Lett. 8, 2–14.
Cooch, E., White, G., 2006. Program MARK: a gentle introduction. Available in. pdf format for free download at http://www.phidot.org/software/mark/docs/book.
Courchamp, F., Clutton-Brock, T., Grenfell, B., 1999. Inverse density dependence and the Allee effect. Trends Ecol. Evol. 14, 405–410.
Curtis, J., Naujokaitis-Lewis, I., 2008. Sensitivity of population viability to spatial and non-spatial parameters using GRIP. Ecol. Appl. 18, 1002–1013.
Ergon, T., Gardner, B., 2014. Separating mortality and emigration: modelling space use, dispersal and survival with robust-design spatial capture–recapture data. Methods Ecol. Evol. 5, 1327–1336.
Flanders-Wanner, B.L., White, G.C., McDaniel, L.L., 2004. Validity of prairie grouse harvest age ratios as production indices. J. Wildl. Manag. 68, 1088–1094.
Fordham, D.A., Akçakaya, H.R., Brook, B.W., Rodriguez, A., Alves, P.C., Civantos, E., Trivino, M., Watts, M.J., Araujo, M.B., 2013. Adapted conservation measures are required to save the Iberian lynx in a changing climate. Nat. Clim. Chang. 3, 899–903.
Francis, C.M., Barker, R.J., Cooch, E.G., 2014. Modelling demographic processes in marked populations: proceedings of the EURING 2013 analytical meeting. Methods Ecol. Evol. 5, 1265–1268.
Gilroy, J.J., Virzi, T., Boulton, R.L., Lockwood, J.L., 2012. A new approach to the "apparent survival" problem: estimating true survival rates from mark–recapture studies. Ecology 93, 1509–1516.
Goodman, L.A., 1960. On the exact variance of products. J. Am. Stat. Assoc. 55, 708–713.
Gould, W.R., Nichols, J.D., 1998. Estimation of temporal variability of survival in animal populations. Ecology 79, 2531–2538.
Halkin, S.L., Linville, S.U., 1999. Northern Cardinal (*Cardinalis cardinalis*). The Birds of North America Online. Cornell Lab of Ornithology, Ithaca, NY, USA (Available: http://bna.birds.cornell.edu/bna/species/440).
Hines, J.E., Kendall, W.L., Nichols, J.D., Thompson III, F., 2003. On the use of the robust design with transient capture–recapture models. Auk 120, 1151–1158.
Huggins, R.M., 1989. On the statistical analysis of capture experiments. Biometrika 76, 133–140.
Huggins, R.M., 1991. Some practical aspects of a conditional likelihood approach to capture experiments. Biometrics 47, 725–732.
Jolly, G.M., 1965. Explicit estimates from capture–recapture data with both death and immigration-stochastic model. Biometrika 52, 225–247.
Keith, D.A., Akçakaya, H.R., Thuiller, W., Midgley, G.F., Pearson, R.G., Phillips, S.J., Regan, H.M., Araújo, M.B., Rebelo, T.G., 2008. Predicting extinction risks under climate change: coupling stochastic population models with dynamic bioclimatic habitat models. Biol. Lett. 4, 560–563.
Kendall, W.L., Nichols, J.D., 1995. On the use of secondary capture–recapture samples to estimate temporary emigration and breeding proportions. J. Appl. Stat. 22, 751–762.
Kendall, W.L., Pollock, K.H., Brownie, C., 1995. A likelihood-based approach to capture–recapture estimation of demographic parameters under the robust design. Biometrics 293–308.
Kendall, W.L., Nichols, J.D., Hines, J.E., 1997. Estimating temporary emigration using capture–recapture data with Pollock's robust design. Ecology 78, 563–578.
King, R., 2012. A review of Bayesian state-space modelling of capture–recapture–recovery data. Interf. Focus 2, 190–204.
Laake, J., 2013. RMark: an R interface for analysis of capture–recapture data with MARK. AFSC Processed Rep 2013-01. Alaska Fish. Sci. Cent., NOAA, Natl. Mar. Fish. Serv 7600 (25 pp.).
Lande, R., 1993. Risks of population extinction from demographic and environmental stochasticity and random catastrophes. Am. Nat. 142, 911–927.
Lindberg, M.S., 2012. A review of designs for capture–mark–recapture studies in discrete time. J. Ornithol. 152, 355–370.
Lunn, D.J., Thomas, A., Best, N., Spiegelhalter, D., 2000. WinBUGS—a Bayesian modelling framework: concepts, structure, and extensibility. Stat. Comput. 10, 325–337.
McCarthy, M.A., Keith, D., Tietjen, J., Burgman, M.A., Maunder, M., Master, L., Brook, B.W., Mace, G., Possingham, H.P., Medellin, R., 2004. Comparing predictions of extinction risk using models and subjective judgement. Acta Oecol. 26, 67–74.
Morris, W., Doak, D., 2002. Quantitative Conservation Biology: Theory and Practice of Population Viability Analysis. Sinauer and Associates. Inc. Publishers, Sunderland, MA.
Nichols, J.D., Hines, J.E., Lebreton, J.-D., Pradel, R., 2000. Estimation of contributions to population growth: a reverse-time capture–recapture approach. Ecology 81, 3362–3376.
Nott, M.P., DeSante, D.F., Scott, J., Heglund, P., Morrison, M., 2002. Demographic monitoring and the identification of transients in mark–recapture models. Predicting Species Occurrences: Issues of Accuracy and Scale. Island Press, Washington, DC, USA, pp. 727–736.
Pearson, R.G., Stanton, J.C., Shoemaker, K.T., Aiello-Lammens, M.E., Ersts, P.J., Horning, N., Fordham, D.A., Raxworthy, C.J., Ryu, H.Y., McNees, J., Akçakaya, H.R., 2014. Life history

and spatial traits predict extinction risk due to climate change. Nat. Clim. Chang. 4, 217–221.
Peery, M.Z., Becker, B.H., Beissinger, S.R., 2007. Age ratios as estimators of productivity: testing assumptions on a threatened seabird, the marbled murrelet (*Brachyramphus marmoratus*). Auk 124, 224–240.
Pradel, R., 1996. Utilization of capture–mark–recapture for the study of recruitment and population growth rate. Biometrics 703–709.
Pradel, R., Hines, J.E., Lebreton, J.-D., Nichols, J.D., 1997. Capture–recapture survival models taking account of transients. Biometrics 53, 60–72.
R Core Team, 2014. R: A Language and Environment for Statistical Computing. R Foundation for Statistical Computing, Vienna, Austria (URL http://www.R-project.org/).
Sauer, J., Hines, J., Fallon, J., Pardieck, K., Ziolkowski, D., Link, W., 2014. The North American breeding bird survey, results and analysis 1966–2012, version 02.19. 2014. US Geological Survey. Patuxent Wildlife Research Center, Laurel, Maryland, USA.
Schaub, M., Abadi, F., 2011. Integrated population models: a novel analysis framework for deeper insights into population dynamics. J. Ornithol. 152, 227–237.
Schaub, M., Kéry, M., 2012. Combining information in hierarchical models improves inferences in population ecology and demographic population analyses. Anim. Conserv. 15, 125–126.
Schaub, M., Royle, J.A., 2014. Estimating true instead of apparent survival using spatial Cormack–Jolly–Seber models. Methods Ecol. Evol. 5, 1316–1326.
Smith, R., Hatch, M., Cimprich, D., Moore, F., Poole, A., 2011. Gray Catbird (*Dumetella carolinensis*). The Birds of North America Online. Cornell Lab of Ornithology, Ithaca, NY, USA (Available: http://bna.birds.cornell.edu/bna/species/167).
Sturtz, S., Ligges, U., Gelman, A.E., 2005. R2WinBUGS: a package for running WinBUGS from R. J. Stat. Softw. 12, 1–16.
White, G.C., Burnham, K.P., 1999. Program MARK: survival estimation from populations of marked animals. Bird Study 46, S120–S139.
Williams, B.K., Nichols, J.D., Conroy, M.J., 2002. Analysis and Management of Animal Populations. Academic Press.
Wilman, H., Belmaker, J., Simpson, J., de la Rosa, C., Rivadeneira, M.M., Jetz, W., 2014. EltonTraits 1.0: species-level foraging attributes of the world's birds and mammals. Ecology 95 2027.